Romanian Journal of Mechanics
Volume 5, Issue 1/2020, pp 15-30, ISSN 2537 - 5229, *rjm.journals.srmta.ro*

NUMERICAL AND EXPERIMENTAL INVESTIGATIONS OF THE BEHAVIOUR OF A FRAME EQUIPPED WITH NITI WIRES. PART 2. THE CASE WITH NITI WIRES

Cristian RUGINĂ [*] , Ligia MUNTEANU [*] , Luciana MAJERCSIK [**] , Ciprian DRAGNE [*]

[*] Institute of Solid Mechanics, Romanian Academy, Bucharest
[**] Transilvania University of Brasov

Corresponding author: Cristian RUGINĂ, E-mail: rugina.cristian@imsar.ro

Abstract: Numerical and experimental analysis on the vibrations of a two-level frame structure equipped/or not with shape memory alloy (SMA) wires is presented in this study. Thise second part of the study, the present article treats the frame equiped with NITi wires. The structural model consists of 2 level structure with constant height of 350 mm and the width of each plate 300 mm. The plates are made out of plexiglass plates to create a rigid plan system and the columns are circular hollow brass rods of diameter 4.00 mm and thickness of 0.40 mm. The sensors are positioned slightly different from the first part, the previous paper. Vibration system tests are performed in order to investigate the behavior of the frame equipped or not with NiTi wires and the effect on the SMA wires on the measured signal shape and amplitudes. Explanations of the the transformation behavior of wires during the experimental tests are given. Numerical finite element method (FEM) simulations are also done in the case without and with NiTi wires heated strongly with an electrical current in order to have a comparison with experimental results.

Key words: Shape-memory alloys, experimental data, seismic protection devices, earthquake engineering.

1. INTRODUCTION

The shape memory alloys (SMA) have the property of changing the shape, the natural frequency and the mechanical properties of a structure by providing a source such as temperature, stress, electrical field or magnetic field [1-3]. The SMA can be used as actuators, sensors to control the dynamical behavior of a structure by embedding them into the structure [4]. Extended overviews of the applications on SMA with are given in [4,6,10,14]. The SMA has two remarkable properties namely: shape memory effect and superelasticity. When the structure is mechanically loaded below the martensite finish temperature, it regains its original shape after removing the loading by heating the structure above the austenite finish temperature. This phenomenon is known as the shape memory effect. The superelasticity is the reversible response to the load caused by phase transformation.

In the 1960s were developed some nickel-titanium alloys with a composition of 53-57% nickel by weight, that exhibited an unusual effect: the deformed specimens with residual strains of 6-10% regained their original shape after a thermal cycle. This effect became as the shape-memory effect. Shape memory alloys (SMA) are materials capable of very large recoverable inelastic strain (of the order of 10%) [7,8]. Numerous works have been done in the area of using NiTi for vibration and mechanical characterization with and without embedding into different types of composites [11-13]. Researchers have been used different diameters of SMA wire, composition, different environment condition etc. However, there is scope for investigation on improvisation of SMA properties with

structure by experimental, numerical and/or analytical techniques.

It is known the application of the shape memory alloy in earthquake engineering as both vibration control and isolation elements for buildings and bridges [9, 14-16]. The Basilica of St. Francis in Assisi, Italy damaged during the 1999 earthquake was restored maintaining the original concept of the structure by connecting the tympanum and the roof by superelastic SMA rods. The SMA rods have the role of reducing the seismic forces transferred to the tympanum [16].

Fugazza [4] tested superelastic NiTi wires and bars on a structure similar with the one used by us in this paper. He focused on the behavior of such elements and performed tests on a random vibration, earthquake like, tests in time domain and recorded accelerations and compared with numerical results.

The SMA performances in control vibrations and earthquake engineering, such as damping properties, material strength and recentering capability are discussed in [17-19].

SMAs are a group of metallic alloys that can return to their original form (shape or size) when subjected to a memorisation process between two transformation phases, which is temperature or magnetic field dependent. This transformation phenomenon is known as the shape memory effect (SME).

The source of the mechanical behavior of SMAs is a crystalline phase transformation between the austenite and martensite. Martensitic structure is obtained from austenite with application of mechanical load or decrease in temperature. Upon heating or reduction of stress, the austenitic structure is recovered.

As the SMA with NiTi wires are so complex materials extended experimental fine tuned researches have been done to characterize them [21,22].

The main object of this study is the experimental investigation of the vibration system tests of a 2-level frame structure equipped with shape memory alloy wires. The frame was vibrated in a wide range of frequencies, and NiTi wires were heated with various current intensities at low and high temperatures. Some comparisons with numerical FEM results will be provided.

2. EXPERIMENTAL SETUP

The experimental setup (Fig.1) consists of a 2 level frame structure, the vibration system, and a data acquisition system measuring the displacements of the structure at different vibration frequencies, for a configuration of sensor positions (Fig.2) different from the one taken in [5].

The structure consists (Fig.3) of two-level frame made of plexiglass supported by hollow brass rods and an additional plexiglass level (level 0) that attach the structure to the vibration system, providing also the stability for the supporting rods. The plexiglass plates were positioned at level of 350mm high one from another. Additional steel plates were attached with screws to the plexiglass plates to give a more realistic approach of weight of real existing structures. The steel plates have been manufactured to weight 0.5 kg each, with geometric dimensions of 160mm×80mm×6.2mm. The geometric dimensions of the plexiglass plates are 300mm×300mm×4mm, with different holes for the supporting rods and additional steel plates, and in future work NITI wires. The supporting rods are positioned to 40mm of the plexiglass plates edges, and not less, to ensure that during the vibrations the plexiglass will not break. The geometric dimensions of the supporting hollow brass rods are the exterior diameter of 4mm and the inner diameter of 3.2mm. The total length of the rods is 1m, the purchased length, and kept so, for subsequent experiments, that will support additional plates of plexiglass.

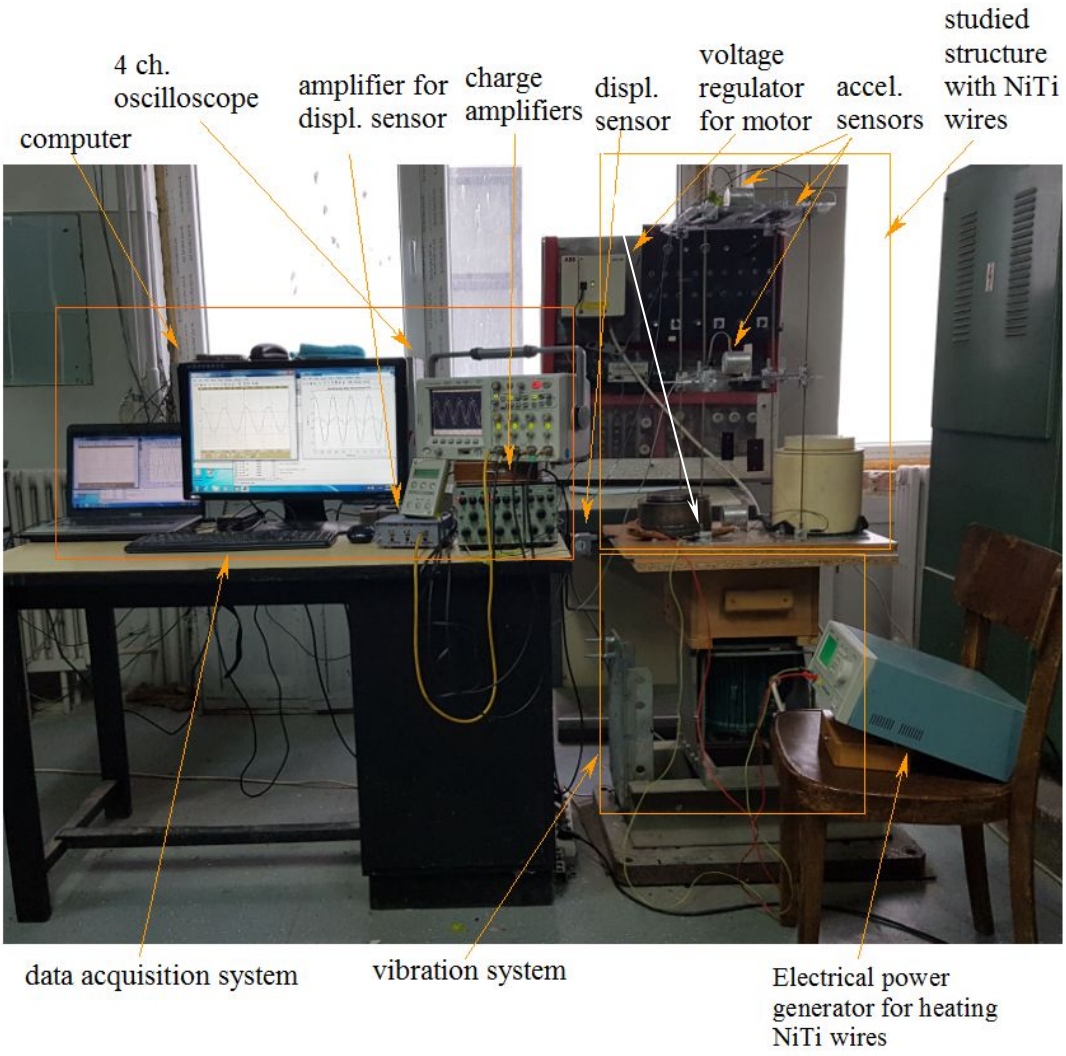

Fig.1 Experimental setup.

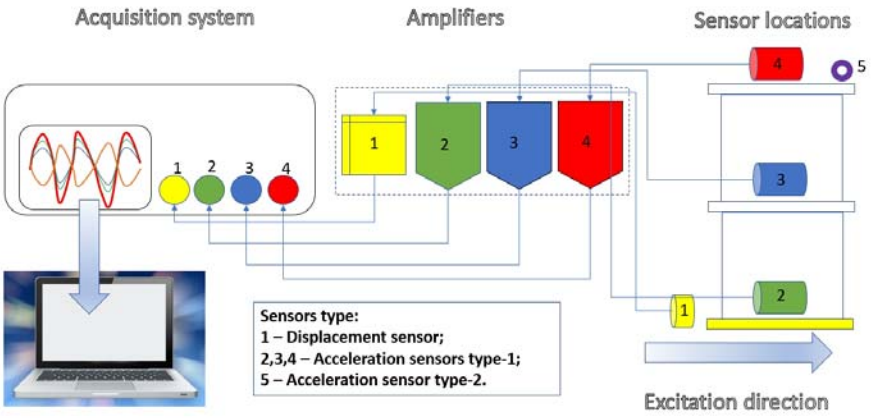

Fig. 2. Schematic diagram of the experimental data acquisition system with sensors.

To ensure that the supporting rods will not collapse during the vibrations, as well as a precision mounting of the plexiglass plates, stiffener assemblies (Fig. 7) made up of washers and nuts were used to attach the plexiglass plates to supporting rods.

In the experimental determinations with NiTi wires, the structure was additionally equipped with fastening elements of NiTi wires (Fig.8) with the possibility to prestress wires in a "guitar string" mode. The NiTi wires were mounted diagonally on two parallel faces of the structure on each level (Fig.3a,c).

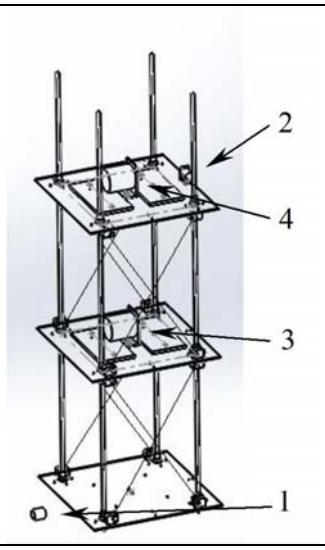

(a)

(b)

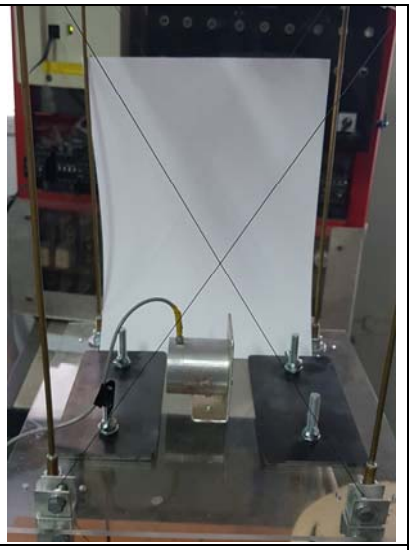

(c)

Fig. 3. Configuration of sensor locations connected to 1,2,3,4 channels of the oscilloscope and NiTi wires mounted to the structure.

Fig.4. Bruel&Kaer Charge Amplifiers Type 2635

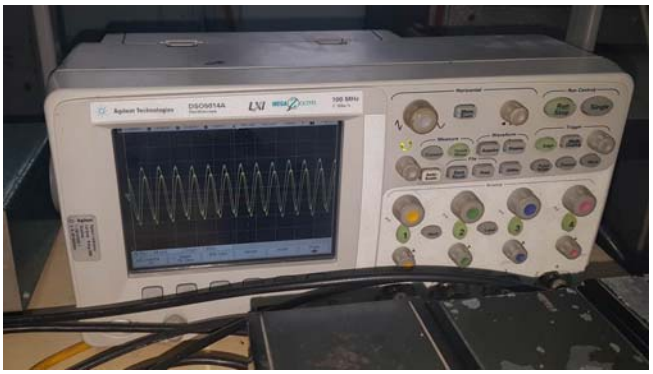

Fig.5. Acquisition system oscilloscope Agilent 5014A

(a)

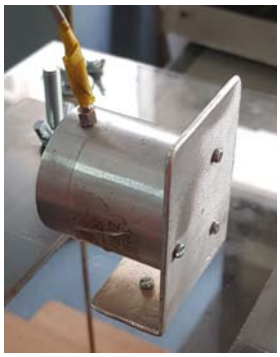

(b)

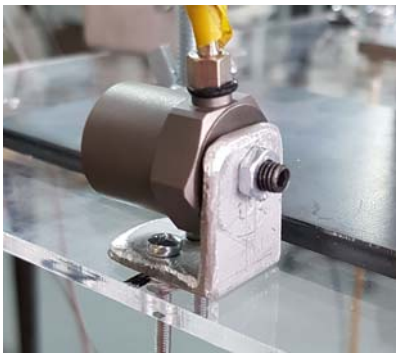

(c)

Fig.6. (a) displacement sensor, (b) accelerometer Type1 (c) accelerometer Type 2.

Fig. 7. Stiffener with washers and nuts

Fig.8. NiTi wire fastener

Fig.9. Electrical power generator

The vibration system (Fig. 1) consists of a wooden table, with additional masses, mounted on parallel very flexible steel plates, that support large deflections, to ensure minimal structural losses in the vibration system, that would be important otherwise, due to friction, in the case of a sliding system. The wooden table is excited by an electric motor with eccentric masses attached, controlled by an ABB ACS-300 AC drives for speed control. The vibrations frequencies are controlled both by the rotational speed of the electric motor and the eccentric masses attached to it.

The displacements measuring system (Fig.1, Fig.2) consists of displacements and acceleration sensors, amplifiers with integration facilities, and an oscilloscope connected to a computer for data acquisition. One displacement sensor of type Celesco SP2-4 was used as a permanent reference of the displacements measured on the base of the structure and connected to the vibration system. Other 3 acceleration sensors, named usually accelerometers, were used to measure the displacements in various points of the vibrating structure by integration of the accelerations with amplifiers having integration facilities. Returning to the accelerometers, we specify that one is of type Bruel&Kaer Charge Accelerometer 4381, and named by us Type2 along this paper, and the others 2 are of type HMF KB12, and named by us Type1. The 3 amplifiers with integration facilities are Bruel&Kaer Charge Amplifier type 2635. The oscilloscope used was an Agilent DSO5014A, with 4 channels, 300MHz bandwidth on 16 bits. The first channel was used to connect to the displacement sensor and used as a reference signal for the others. For the remaining 3 channels, accelerometers were used (Fig.3).

The NiTi wires were mounted diagonally on two parallel faces of the structure on each level (Fig.3.a,c), and heated by a continuous electrical current given by a power source (Fig.9). The NiTi wires are 39 cm long and electrically mounted in series.

3. EXPERIMENTAL MEASUREMENTS

As the experimental determinations of calibration of the measurement system and evaluation of the structural damping and determination of free vibrations resonance frequency was done in the fist part of the study [5], we focused our attention on the behavior of the NiTi wires on the resonance modes and frequencies of the enhanced structure.

First a short survey of the NiTi wires SMA is presented in order to explain the measured experimental data obtained.

Practically, SMAs can exist in two different phases with three different crystal structures (i.e. twinned martensite, detwinned martensite and austenite) and six possible transformations [6] (see Fig.10.a). The austenite structure is stable at high temperature, and the martensite structure is stable at lower temperatures. When a SMA is heated, it begins to transform from martensite into the austenite phase. The austenite-start-temperature (As) is the temperature where this transformation starts and the austenite-finish-temperature (Af) is the temperature where this transformation is

complete. Once a SMA is heated beyond As it begins to contract and transform into the austenite structure, i.e. to recover into its original form. This transformation is possible even under high applied loads, and therefore, results in high actuation energy densities [6]. During the cooling process, the transformation starts to revert to the martensite at martensite-start-temperature (Ms) and is complete when it reaches the martensite-finish-temperature (Mf).

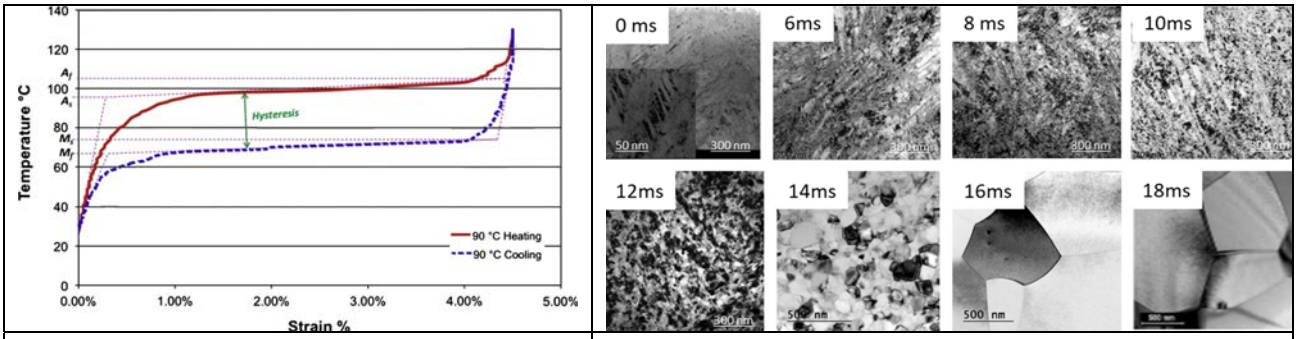

Fig. 10. (a) Phase transformation (martensite-austenite) of NiTi SMA [6], and (b) crystaline structure during phase transformation when heating with high power electrical pulse [21].

However this thermal hysteretic behaviour is only theoretical. In real experiments the crystalline structure of SMA NiTi wires both in martensite and austenite state exhibits significant degradations after large deformations or large temperature differences, or a simultaneous combination of them [21],[22].

When an external stress is applied below the martensite yield strength (approximately 8.5% strain for NiTi alloys [6]), the SMA deforms elastically with recoverable strain. However, a large non-elastic deformation (permanent plastic deformation) will result beyond this point. Most applications will restrict the strain level; e.g. to 4% or less, for NiTi alloys [6].

Fig. 11. NiTi crystalline structure degradation after 20 cycles according to [22].

Usually the NiTi wires are heated with pulse electrical current. Application of pulse times longer than 22 ms with power density 160 W/mm3 causes rapid oxidation, even at short millisecond times, which severely damages the wire [22]. An extesive experimetal study has been done [22], with specialized controlled and measurement capabilities including a Transmission Electron Microscopy (TEM) to visually study the crystalline structure of NiTi wires after 20 cycles, and found significant degradations (Fig.11).

In the experimental measurements conducted by Fugazza [4], he applied a random vibration excitation on a system similar to ours. In our experimental measurement we used a constant frequency vibration system and recorded the displacement's amplitude. We swept a frequency range between 1.25 Hz and 8.0 Hz assuming that real earthquake do not exceed the maximum frequency chosen. Also, in our experimental measurement we used continuous electrical current with much less power to avoid overheating the NiTi wires.

The structure without NiTi wires has three vibration modes, as shows in [5] two bending modes and one torsional mode Fig.20b,c,d. The structure with NiTi wires (approximated in FEM

computations as elastodynamic roads without buckling) has only two bending modes in the considered frequency range, at almost the same frequency as without NiTi, but the vibration modes are different. The displacements are perpendicular the excitation direction (Fig.21b,c,d).

A first set of measurements has been done without the NiTi wires, even if in [5] we studied it separately, because a different sensor configuration has been taken into account in this paper, in order to have a reference for the subsequent sets of measurements. The plots of displacements, and relative displacements for this first set of measurements are presented in fig.12a,b. Due to small asymmetries in the structure and in the sensor type 2 (at the edge of the structure fig.3.a), a significant displacement perpendicular (Oy) to the excitation direction (Ox) is present, around 3.6 Hz, even if in FEM computations they do not appear.

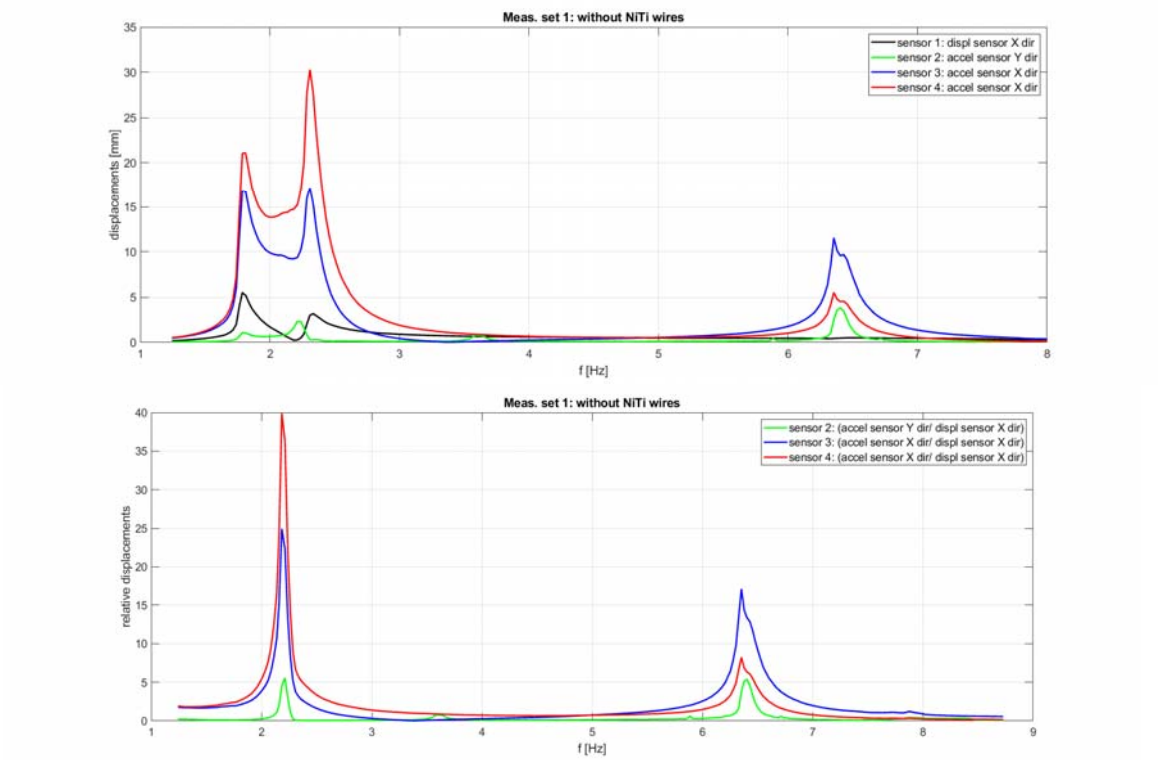

Fig.12. (a) Measured displacements and (b) measured relative displacements in the first set of experimental determinations without NiTi wires.

Next, a second set of measurements has been done with NiTi wires, with weak prestress. The plots of relative displacements for this second set of measurements are presented in Fig.13. After the first resonance the cumulative plastic deformations leads to weakening of the NiTi wires. The vibration amplitudes of sensors 3 and 4 (on the Ox directions) increase slowly around 3.6 Hz, the same resonance as the torsion mode on the structure without NiTi wires. For sensor 2 (on the Oy direction) it can be seen also two distinct resonance peaks around 2.3 Hz and 6.4 Hz the same as in the case without NiTi wires but smaller in amplitudes.

After this second set of measurement the wires were significanlty weakened. So we applied a small electrical current to try to remember the initial shape of the NiTi wires. Even if the shape of austenite cristaline state of the NiTi wires has been temporarely restored during heating, after cooling down the NitTi wires were still weakened, meaning that the plastic deformations exceeded significantly the known 8.5%. Moreover, the number of mechanical vibration cycles were more than the 20 thermal cycles presented above and studied by [22, 22]. That show that the martensite crystaline structure of the NiTi wires was significantly damaged.

Next a third set of measurements has been done. The weakened NiTi wires were pretensioned once again with bigger prestress. The plots of displacements and relative displacements for this set

of measurements are presented in Fig.14. It can be seen that the mechanical fatigue due cycling vibrations caused a sudden change in the crystalline structure of the NiTi wires, before 6 Hz, before the second resonance frequency of 6.4 Hz. After this severe deterioration of the material, by sudden deformation of the material, an effect of mechanical shock, a whipping of the NiTi wires, was observed in the vibrations of the structure. The recorded signals just before and after the sudden degradation are presented in Fig.15.

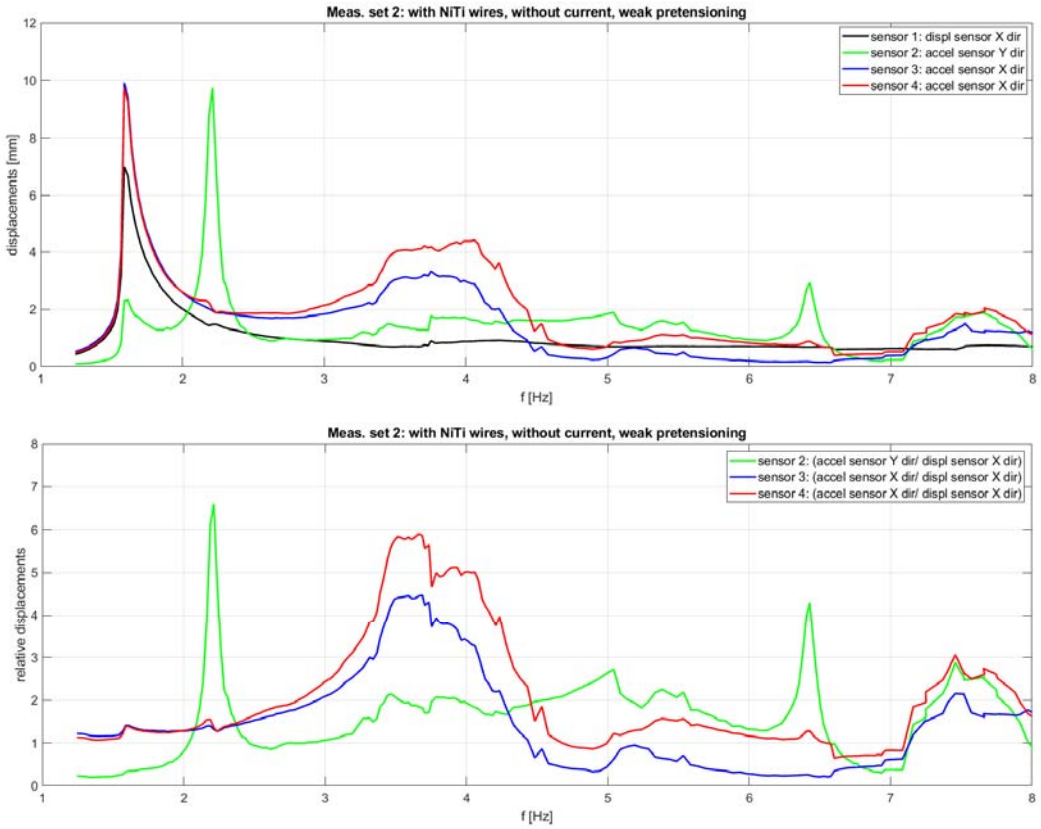

Fig.13. (a) Measured displacements and (b) measured relative displacements in the second set of experimental determinations with NiTi wires, with no electrical current.

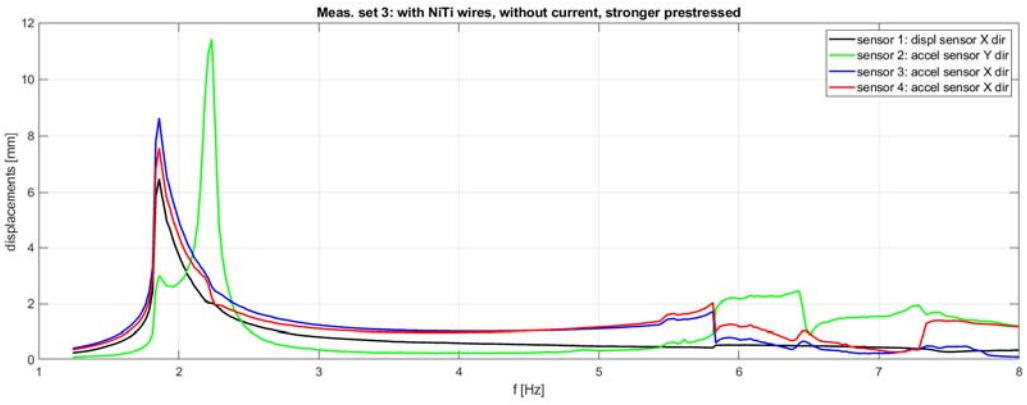

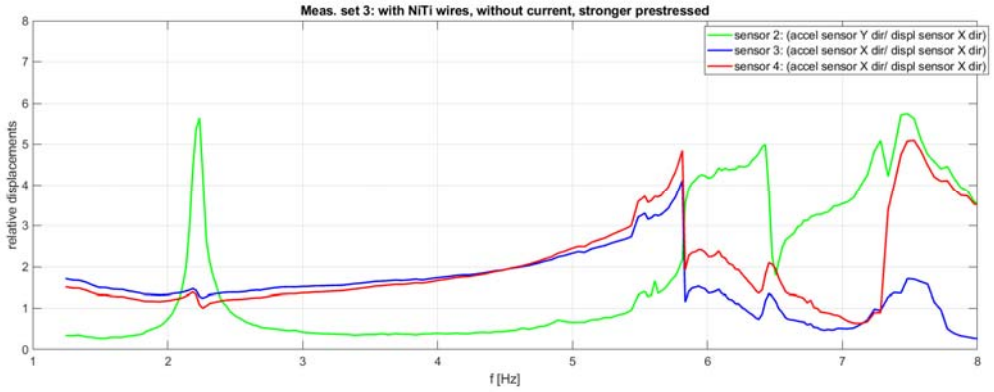

(b)

Fig. 14. (a) Measured displacements and (b) measured relative displacements in the third set of experimental determinations with NiTi wires, with no electrical current.

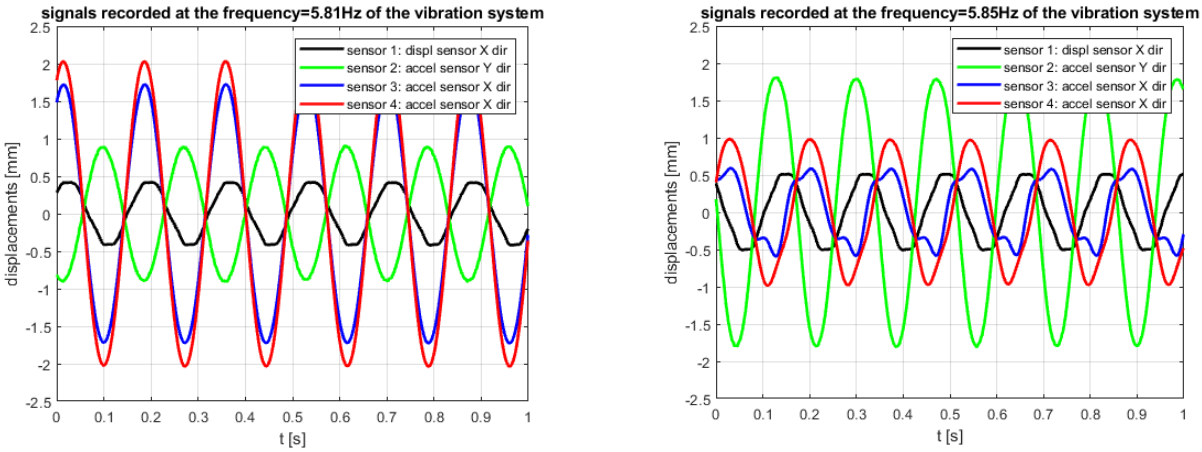

(a) (b)

Fig.15. The recorded signals (a) before and (b) after the sudden degradation presented in Fig.14.

Next a fourth set of measurements has been done. Once again, the weakened NiTi wires were pretensioned with significant prestress. The plots of displacements and relative displacements for this set of measurements are presented in Fig.16. It can be seen that the mechanical fatigue due cycling vibrations caused a sudden change in the crystalline structure of the NiTi wires. much earlier than the previous set of measurements, not at 5.8 Hz but at about 4.5Hz. Shortly after 8 Hz one of the NiTi wires snapped. After replacing the wire and prestressing again all of them, a fifth set of measurements has been done and results presented in Fig.17. It can be observed that the sudden drop in vibration amplitudes was observed at even lower frequencies at 3.9 Hz.

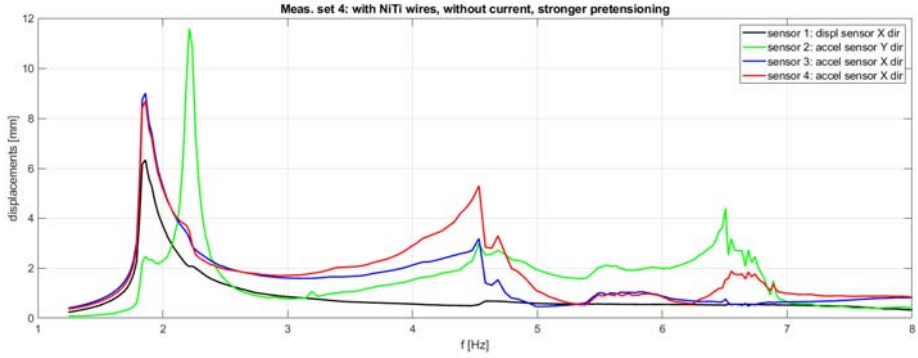

(a)

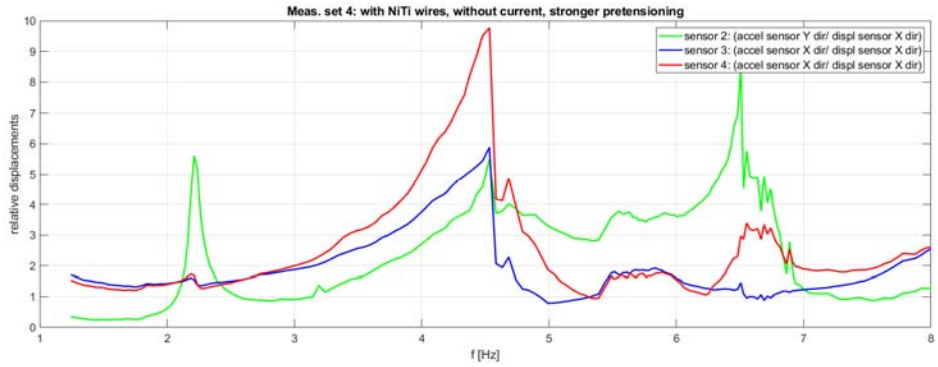

(b)

Fig. 16. (a) Measured displacements and (b) measured relative displacements in the fourth set of experimental determinations with NiTi wires, with no electrical current.

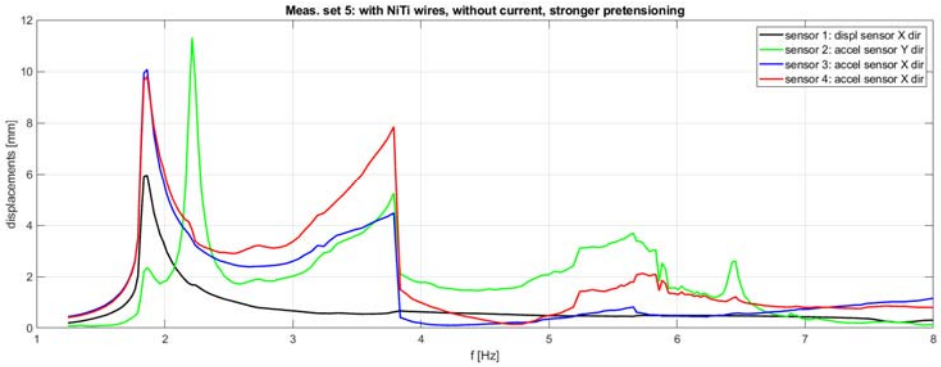

(a)

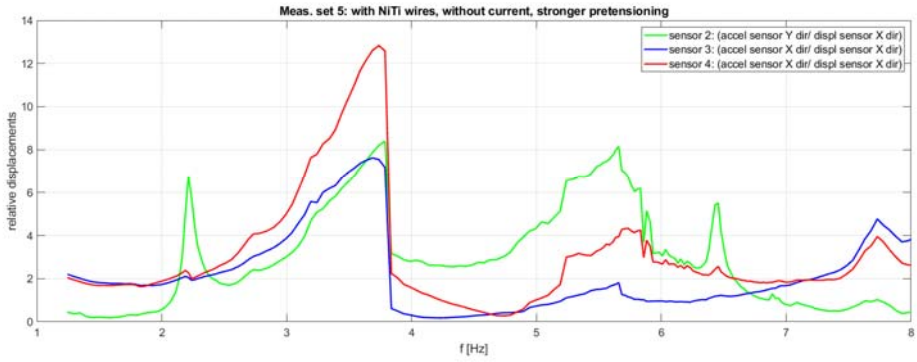

(b)

Fig. 17. (a) Measured displacements and (b) measured relative displacements in the fifth set of experimental determinations with NiTi wires, with no electrical current.

A sixth set of measurements was done with NiTi wires under constant electrical current of 0.65A and a electrical power of about 11W. The plots of displacements and relative displacements for this set of measurements are presented in Fig.18. It can be seen that even with a small heating of the NiTi wires, when a small phase change martensite-austenite in the wires occurred, the wires showed the same behavior of sudden change in vibration amplitude, this time at about 6.2 Hz just before the 6.4 Hz resonance frequency.

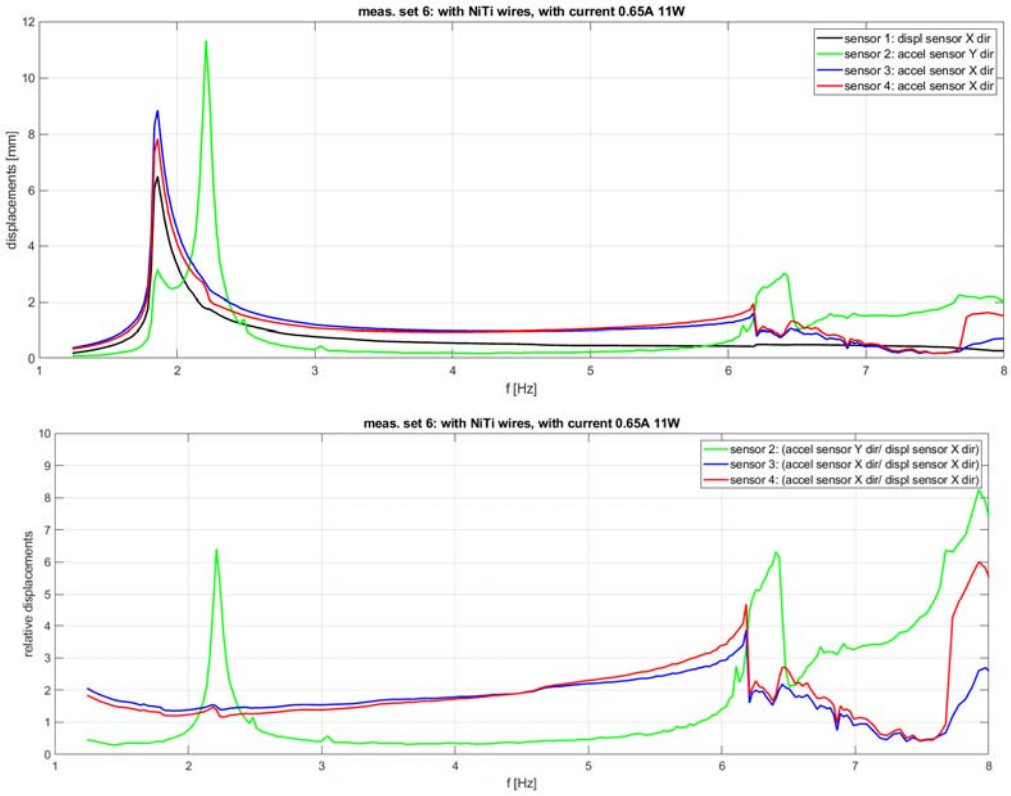

(a)

(b)

Fig.18. (a) Measured displacements and (b) measured relative displacements in the sixth set of experimental determinations with NiTi wires, with electrical current of 0.65 A, 11W.

A seventh set of measurement was done with NiTi wires under constant electrical current of 1.0A and an electrical power of about 17.5W. The plots of displacements and relative displacements for this set of measurements are presented in Fig.19. The wires were strongly prestressed before applying the electrical current and a significant heating was applied to them. In this case no drop in vibration amplitudes was observed. The NiTi wires were in such a high prestress, that no plastic deformations were present. Even so, just before 8Hz another wire snapped (Fig.19b).

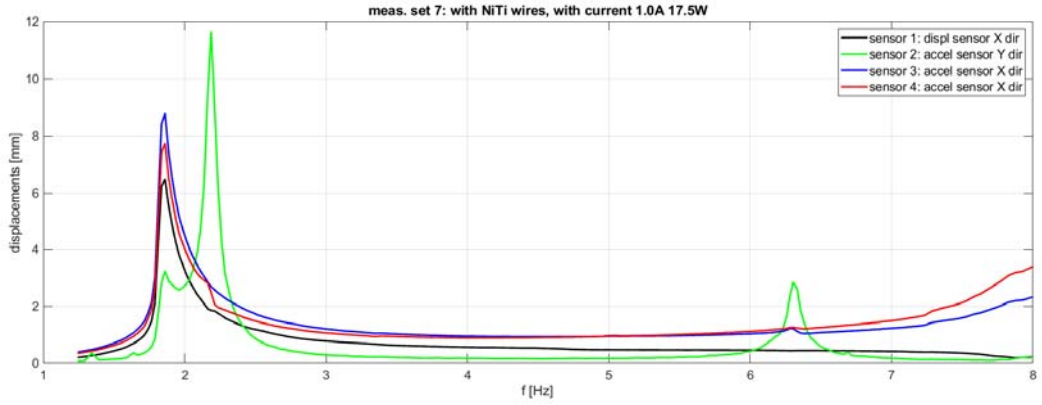

(a)

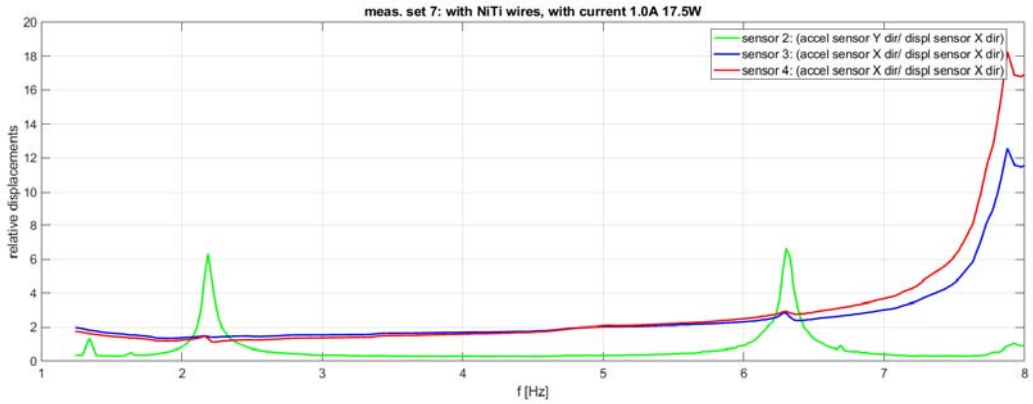

(b)

Fig.19. (a) Measured displacements and (b) measured relative displacements in the seventh set of experimental determinations with NiTi wires, with electrical current of 1.0A, 17.5W.

4. NUMERICAL FEM RESULTS

The FEM computations were done in Comsol 5.3, in both eigenfrequency and frequency domain study, for both configurations of the sensors, with a slightly simplified geometric model (Fig 20a and 21a), to shorten the computational time and resources needed.

The stiffener assemblies made up of washers and nuts in experiments (Fig. 7) were simplified to steel cylinders surrounding the rods around the joints with plexiglass plates. For these simplified stiffeners the geometric dimensions taken in simulations are: outer diameter of 8mm, inner diameter of 4mm and length of 50mm. The Type1 and Type2 sensors were approximated to blocks of aluminum and steel with the same weight as the real ones of 225g, and 55g respectively. The elastic properties of the brass rods were approximated to copper rods. The additional steel plates are considered bonded, and not attached with screws. The NiTi wires were approximated with rods half Ni half Ti, that do not buckle, with diameter of 0.5mm.

The parameters for grid size were taken 'finer' for the brass hollow rods (approximated to copper hollow rods) and steel stiffeners, and only 'fine' for plexiglass plates, steel plates and simplified aluminum 2024 and steel sensors blocks. The structural losses have been considered of 1.3%, as in the experimental determination, in the first part of the study, in the previous paper [5], at the resonance frequency, even it is known that it is not constant for all frequencies, in fact increasing with frequency.

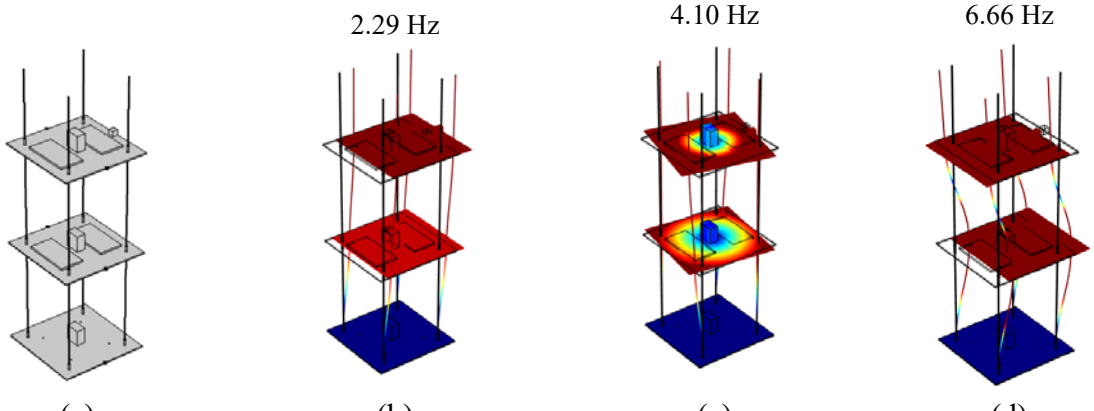

Fig. 20. (a) Simplified geometry taken in FEM computation, (b), (c), (d) computed FEM mode shapes for structure without NiTi wires.

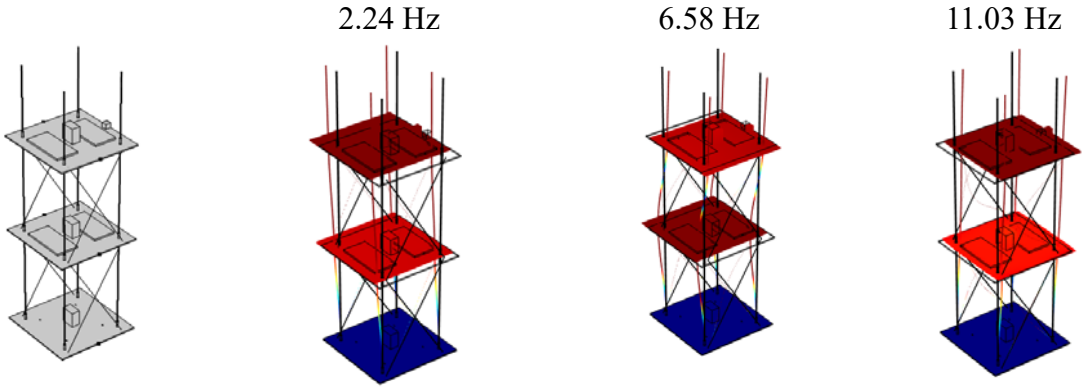

Fig.21. (a) Simplified geometry taken in FEM computation, (b), (c), (d) computed FEM mode shapes for structure with NiTi wires.

The elastic properties of the materials, modulus of elasticity E , Poisson ratio ν , mass density ρ , taken in the FEM simulations are taken mainly from the Comsol 5.3 library, and are

- for copper: $E = 126\,GPa$, $\nu = 0.335$, $\rho = 8940\,kg/m^3$
- for plexiglass: $E = 3.0\,GPa$, $\nu = 0.4$, $\rho = 1190\,kg/m^3$
- for steel: $E = 211.9\,GPa$, $\nu = 0.228$, $\rho = 7860\,kg/m^3$
- for aluminum 2024: $E = 73.14\,GPa$, $\nu = 0.331$, $\rho = 2780\,kg/m^3$
- for NiTi: $E = 62.43\,GPa$, $\nu = 0.33$, $\rho = 6450.0\,kg/m^3$

In the case without NiTi wires the FEM eigenfrequency study shows the presence of 3 vibrations modes, mode 1 and mode 3 for bending modes (Fig.20b,d) and mode 2 for torsion mode (Fig.20c).

In the case with NiTi wires the FEM eigenfrequency study shows the presence of 3 vibrations bending modes (Fig.21b,c,d). The firsts 2 bending modes are at frequencies closed to the bending modes of the structure without wires, but the vibration direction is perpendicular (Oy) to the direction of excitation (Ox). The third bending mode of the structure with wires is similar to the first structure without wires, but is very small and the frequency is far away (11.03 Hz).

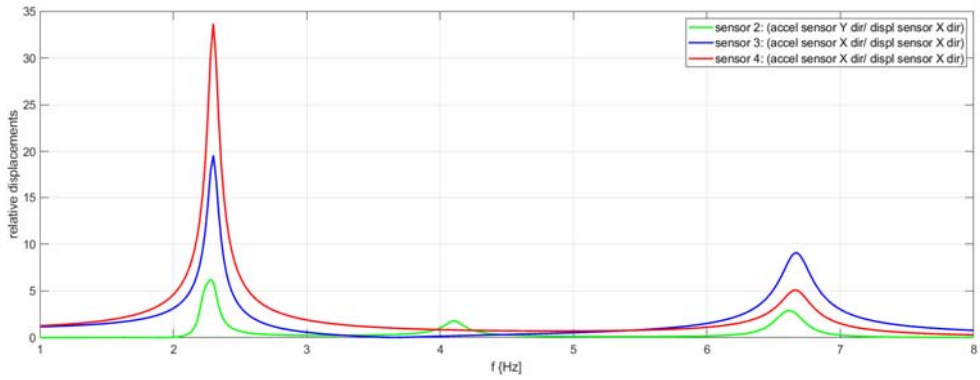

Fig.22. Computed FEM relative displacement for the structure without NiTi wires.

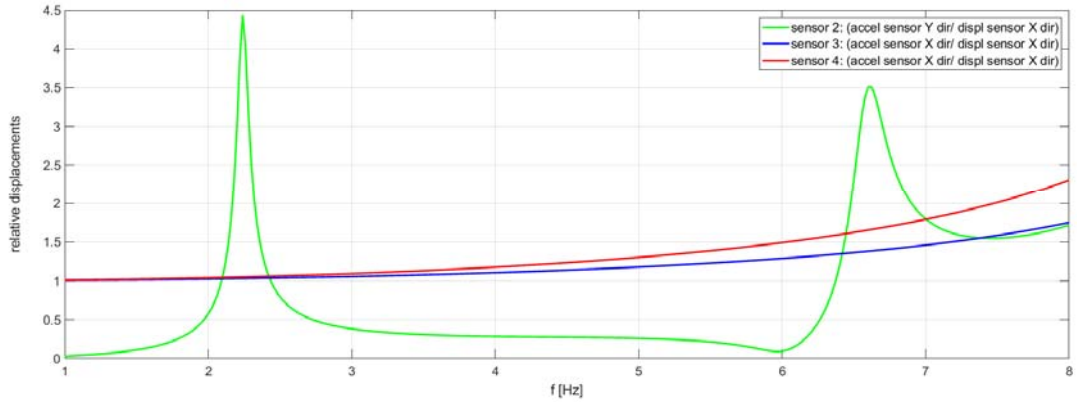

Fig. 23. Computed FEM relative displacement for the structure with NiTi wires.

The FEM frequency study was done for o comparison of the experimental plots Fig.12 and Fig.19 with the numerical ones. The computed frequency domain was 1.0 Hz - 8.0 Hz in steps of 0.02 Hz. The point where the values were computed are the center and middle edges of the plexiglass plates, in close proximity of the sensor's locations. The computed plots in relative values (relative to base displacements) are presented in Fig.22 for the structure without NiTi wires, and in Fig.23 for the structure with NiTi wires. The plots presents the computed relative modulus of displacement (modulus of displacements in sensor position/modulus of displacements of the bottom level) in the sensing direction of the accelerometers: O*x* for Type1 and Oy for Type2: $\sqrt{\mathrm{Re}(u)^2+\mathrm{Im}(u)^2}$ and respectively $\sqrt{\mathrm{Re}(v)^2+\mathrm{Im}(v)^2}$, were *u* and *v* are the computed displacements in the *Ox* and *Oy* directions, both complex values.

For the structure without NiTi wires the computed FEM plots (Fig.22) agree well with the measured experimental plots (Fig.12).

For the structure with NiTi wires the computed FEM plots (Fig.23) agree well with the measured experimental plots (Fig.19) when a high prestress and high electrical current is applied to the NiTi wires.

5. CONCLUSIONS

This paper is the second part of a study concerning the vibration of a structure made of 2 level frames, that includes NiTi wires as passive and active dampers.

Along the conclusions presented in the first part of the study, in the previous paper some conclusions can be remarked.

When large and heavy mechanical cycling is applied to the structure with NiTi wires, cumulative stress and material fatigue on NiTi SMA wires leads to significant degradation of the wires. This can be seen in sudden drop in amplitude of the upper floors of the structure, accompanied by a weakening of the NiTi wires that lead to mechanical shocks and a whipping effect of the wires. If the vibration of the structure continues some of the wires do snapped.

Even when a moderate constant electrical current (0.65A, 11W) is applied, the same phenomenon is observed, but at higher frequencies.

Only when a strong constant electrical current (1.0A, 17.5W) is applied, capable to heat enough the NiTi wires, the stiffness of the structure does not allow mechanical shocks and whipping of the wires.

The bending resonance frequencies do not change but the vibration modes do. The vibration change directions, from along the excitation direction, to perpendicular to the excitation direction, visible in experimental and computed FEM results.

Acknowledgements. The authors thanks to Dr. Tudor Sireteanu, Dr. Veturia Chiroiu and Dr. Iulian Girip for fruitful discussions and meaningful suggestions.

REFERENCES

1. ANDRAWES, B., MCCORMICK, J., DESROCHES, R., *Effect of cycling modeling parameters on the behavior of shape memory alloys for seismic applications,* SPIE Conference on Smart Structures and Materials, 2004.
2. AURICCHIO, F., SACCO, E.,*Thermo-mechanical modelling of a superelastic shape- memory wire under cyclic stretching-bending loadings*, International Journal of Solids and Structures, vol. **38**, pp. 6123–6145, 2001.
3. CORBI, O., *Shape memory alloys and their application in structural oscillations attenuation*, Simulation Modelling Practice and Theory, vol. **11**, pp. 387–402, 2003.
4. FUGAZZA, D., *Shape-memory alloy devices in earthquake engineering: mechanical properties, constitutive modelling and numerical simulations*, Master's thesis, European School of Advanced Studies in Reduction of Seismic Risk (ROSE School) 2003.
5. RUGINĂ, C., DRAGNE, C., GIRIP, I., BALDOVIN, D., MAJERCSIK, L., *Numerical and experimental investigations of the behaviour of a frame equipped with niti wires. part 1. the case of absence of NiTi wires*, Romanian Journal of Mechanics, 4(1), pp 3-14, 2019.
6. MOHD, J., LEARY, M., SUBIC, A., et al., *A review of shape memory alloy research, applications and opportunities*, Mater. Des., 56,1078–1113, 2014.
7. TOBUSHI, H., SHIMENO, Y., HACHISUKA, T., TANAKA, K., *Influence of strain rate on superelastic properties of TiNi shape memory alloy*, Mechanics of Materials, vol. **30**, pp. 141–150, 1998.
8. STRNADEL, B., OHASHI, S., OHTSUKA, H., ISHIHARA, T., MIYAZAKI, S., *Cyclic stress-strain characteristics of Ti-Ni and Ti-Ni-Cu shape memory alloys*, Materials Science and Engineering, vol. **202**, pp. 148–156, 1995.
9. TAMAI, H., KITAGAWA, Y., *Pseudoelastic behavior of shape memory alloy wire and its application to seismic resistance member for building*, Computational Materials Science, vol. **25**, pp. 218–227, 2002.
10. SADAT, S., SALICHS, J., NOORI, M., HOU, Z., DAVOODI, H., BAR-ON, I., SUZUKI, Y., MASUDA, A., *An overview of vibration and seismic applications of NiTi shape memory alloy, Smart Materials and Structures*, vol. **11**, pp. 218–229, 2002.
11. BARZEGARI, M.M., DARDEL, M., FATHI, A., *Vibration analysis of a beam with embedded shape memory alloy wires*, Acta Mech. Solida Sin., **26**, 536–550, 2013.
12. SONG, G., KELLY, B., AGRAWAL, B.N., *Active position control of a shape memory alloy wire actuated composite beam*, Smart Mater. Struct, **9**, 711-716, 2000.
13. NOOLVI, B., RAJA, S., NAGARAJ, S., et al., *Fabrication and testing of SMA composite beam with shape control*, AIP Conference Proceedings 1859, paper 020055, 2017.
14. WILSON, J., WESOLOWSKY, M., *Shape memory alloys for seismic response modification: a state-of-the-art review*, Earthquake Spectra, vol. **21**, pp. 569–601, 2005.
15. WILDE, K., GARDONI, P., FUJINO, Y., *Base isolation system with shape memory alloy device for elevated highway bridges*, Engineering Structures, vol. **22**, pp. 222– 229, 2000.
16. MAZZOLANI, F. M., MANDARA, A., *Modern trends in the use of special metals for the improvement of historical and monumental structures*, Engineering Structures, vol. **24**, pp. 843–856, 2002.
17. MIHAILESCU, M., CHIROIU, V., *Advanced mechanics on shells and intelligent structures*, Publishing House of the Romanian Academy, 2004.
18. CHIROIU, V., IONESCU, M.F., SIRETEANU, T., IOAN, R., MUNTEANU, L., *On intrinsic time measure in the modeling of cyclic behavior of a Nitinol cubic block*, Smart Materials and Structures, **24**(3), 035022 1-11, 2015.
19. CHIROIU, V., MUNTEANU, L., *A flexible beam actuated by a shape memory alloy ribbon*, Proceedings of the Romanian Academy, Series A: Mathematics, Physics, Technical Sciences, Information Science, **4**(1), 45–51, 2003.
20. Brocca, M., Brinson, L.C., Bazzant, Z.P., *Three- dimensional constitutive model for shape memory alloys based on microplane model*, Journal of the Mechanics and Physics of Solids, **50**, p.1051 – 1077, 2002.
21. MALARD, B., PILCH, J., SITTNER, P., DELVILLE, R., CURFS, C., *In situ investigation of the fast microstructure evolution during electropulse treatment of cold drawn NiTi wires*, Acta Materialia, **59,** pp1542-1556, 2011.

22. CHEN, Y., TYC, O., MOLNAROVA, O., HELLER, L., SITTNER, P., *Tensile Deformation of Superelastic NiTi Wires in Wide Temperature and Microstructure Ranges*, Shape Memory Superelasticity **5**, pp.42–62, 2019.
23. IOAN, R., MUNTEANU, L., DUMITRIU, D., *Determination of Dynamic Young's Modulus Young's Modulus for Steel Alloys,* Romanian Journal of Mechanics, **1**(1), 3-12, 2016.

Received September 12, 2019